buildings

MDPI

Article

A Unified Winkler Model for Vertical and Lateral Dynamic Analysis of Tapered Piles in Layered Soils in the Frequency Domain

Qiangqiang Shua [1], Huanliang Xu [2], Wenbo Tu [2,*], Mingkang Li [3] and Ningzhuo Shi [1]

[1] School of Architectural Engineering, Sichuan University of Arts and Science, Dazhou 635000, China
[2] Engineering Research Center of Railway Environmental Vibration and Noise, Ministry of Education, East China Jiaotong University, Nanchang 330013, China
[3] Xizang Boshi Engineering Design Co., Ltd., Chengdu 610095, China
* Correspondence: wenbotu@ecjtu.edu.cn

Abstract: Tapered piles are a new type of pile foundation known for their simple construction and high bearing capacity, commonly used in railway, highway, or building foundation treatment. This study proposes a unified dynamic Winkler model for vertical and lateral vibration response of tapered piles in the frequency domain using the impedance function transfer matrix method. The computational expressions are obtained for the different springs and damping of tapered piles with different dimensions using the elastodynamic theoretical of rigid embedded foundations, and the dynamic interaction mechanisms of vertical and lateral vibrations between tapered piles and soil are analyzed. The rationality of the simplified model is validated by comparison with existing literature and finite element simulation results. Finally, an example is provided to discuss the influences of the dimensional parameters of the pile and soil properties on vertical, lateral, and rocking dynamic impedance. The analytical findings demonstrate that the lateral and rocking dynamic impedances of tapered piles undergo a substantially greater enhancement relative to their vertical counterpart as the taper angle is progressively enlarged, assuming the pile volume remains constant. The dynamic impedance of tapered piles under vertical and lateral vibration in upper hard and lower weak soil layers, or upper weak and lower hard soil layers, are both greater than those in a homogeneous foundation. Specifically, the vertical dynamic stiffness of tapered piles in double-layered soils is approximately twice that of homogeneous soil. The rocking dynamic stiffness of the pile is significantly influenced by the soil properties around the pile foundation, whereas the soil properties have little impact on the rocking damping coefficient. Overall, the vertical dynamic characteristics are less influenced by the geometric features of the upper part of the tapered pile, while the lateral dynamic characteristics are significantly affected by these features. The lateral dynamic impedance of the tapered pile increases with the diameter of the upper part of the pile. Furthermore, the vertical, lateral, and rocking dynamic impedance of the pile can be effectively improved by enhancing the soil properties around its upper section. These results can provide theoretical references for the engineering practice.

Keywords: tapered pile; dynamic; layered soil; frequency domain

Academic Editor: Nerio Tullini

Received: 17 January 2025
Revised: 18 February 2025
Accepted: 18 February 2025
Published: 20 February 2025

Citation: Shua, Q.; Xu, H.; Tu, W.; Li, M.; Shi, N. A Unified Winkler Model for Vertical and Lateral Dynamic Analysis of Tapered Piles in Layered Soils in the Frequency Domain. *Buildings* **2025**, *15*, 651. https://doi.org/10.3390/buildings15050651

1. Introduction

Tapered piles, characterized by a cross-section that decreases in diameter from top to bottom along a linear variation with depth, represent an innovative cylindrical foundation

type widely applied in railway, highway, or building foundation treatment. The tapered pile has the characteristics of simple construction and high bearing capacity. Studies have shown that compared to cylindrical piles of equal volume, tapered piles exhibit a 0.5–2.5-fold enhancement in vertical load-bearing capacity [1–3] and lateral load-bearing capacity by 0.6 to 0.8 times [4,5]. However, the above-mentioned research mostly emphasized the static loading properties of tapered piles. The tapered pile foundation used in subgrade engineering or bridge engineering is always affected by traffic, wind, and wave load for a long time, all of which are dynamic loads in the field. Specifically, the piles in the subgrade not only bear the vertical traffic load and reduce the settlement of the foundation, but also play a role of vertical and lateral vibration isolation. Therefore, the lateral and vertical vibration characteristics of tapered piles are crucial considerations when pile foundations are subjected to dynamic traffic loads [6,7].

The vertical dynamic response of tapered piles has been investigated through diverse theoretical frameworks. Specifically, Saha and Ghosh [8] proposed a finite difference-based methodology to investigate the axial vibration response of tapered concrete piles, emphasizing the length–diameter ratio, soil Poisson's ratio, and taper angle influencing the vertical dynamic properties. Wu et al. [9] and Wang et al. [10] developed analytical solutions for vertically vibrating tapered piles using the plane strain model and Rayleigh–Love rod theory. And the effects of constraints of pile end, design, and material parameters of tapered piles on the vertical dynamic response also be investigated [9,11]. Hu et al. [12] and Shua et al. [13] introduced a simplified calculation method to identify the vertical dynamic response of the tapered pile and studied the effects of pile length, taper angle, and pile diameter on the dynamic stiffness, damping, and resonant frequency of piles with the same volume.

Tapered piles are primarily used to withstand lateral loads in engineering applications, such as foundation pits, slope stabilization, and offshore platforms. However, relatively few studies have been performed on the lateral bearing analysis of tapered piles, especially in terms of lateral dynamics. Ghazavi [14] performed an investigation of the kinematic seismic response of tapered piles due to earthquakes, where one-dimensional wave propagation theory was used to calculate the lateral free-field displacement of the soil. The results demonstrate that tapered piles exhibit significantly higher energy dissipation susceptibility under seismic excitation compared to uniform-section piles of equivalent volumetric conditions. Dehghanpoor and Ghazavi [15] obtained the harmonic vibration properties of the tapered pile and the influence of soil properties and loading conditions between pile and soil were investigated based on the simplified analytical model. Yang [16] analyzed the vibration behavior of tapered piles under lateral loading embedded in a viscoelastic foundation using the Timoshenko beam model. Zhou et al. [17] derived a simplified equation for the lateral deformation of the tapered pile under harmonic loading by modeling the soil body as a number of springs along the pile shaft in accordance with the Winkler foundation model.

Although existing research have proposed different computational approaches for the vibration response analysis of tapered piles and obtained good results, it can be observed that the analytical theories and computational methodologies for the dynamic responses of tapered piles under vertical and lateral loadings seem to be independent and unrelated, which clearly hinders the design and widespread application of tapered piles. On the other hand, the tapered pile has been modeled as cylindrical segments with varying diameters, the calculation process is the same as the traditional cylindrical pile and it fails to incorporate the dynamic interaction between the inclined surfaces of tapered piles and surrounding soil, which significantly influences their vertical and lateral dynamic

responses. Consequently, comprehensive investigations into pile–soil interaction remain warranted to establish refined design criteria for tapered pile foundations.

The purpose of this study is to present a unified analytical model for the dynamic properties of tapered piles under vertical or lateral loadings, accompanied by considerations of the dynamic interaction between the pile and soil. To effectively account for the mechanical characteristics of tapered piles, the dynamic responses of tapered piles embedded in layered soils under vertical and lateral loadings were investigated using the four-springs dynamic Winkler model and the impedance function transfer matrix approach. The results are compared with the existing analytical solutions and finite element simulations. Finally, through an example, the effects of dimensional design parameters of tapered piles and the layered soil properties on the vertical and lateral dynamic impedance of the pile are discussed, which provides a theoretical reference for the engineering practice.

2. Analyzing the Vertical Dynamic Characteristics of Tapered Piles in Layered Soils

The dynamic Winkler model can effectively simulate the radiation damping effect and inertial coupling mechanisms of the soil surrounding piles through a distributed spring-damper system [18]. Meanwhile, the recursive nature of the transfer matrix method inherently aligns with the continuously varying cross-sectional characteristics of tapered piles [8]. By employing a piecewise homogenization approach, the problem of solving vibration partial differential equations is reduced to the computation of impedance function transfer matrices while maintaining computational accuracy. Therefore, this study adopts the dynamic Winkler model and impedance function transfer matrix method to perform dynamic analysis of tapered piles.

The computational model adopts Winkler's dynamic formulation, wherein the pile satisfies three criteria: vertical, linear elastic, and fully bonded to the soil. Assuming the tapered pile with a taper angle θ, pile length L, and pile end diameter d are subjected to a sinusoidal steady excitation $Ve^{i\omega t}$, the pile must account for the combined action of the shear and normal force due to the slope of the pile shaft which is different from the equal diameter pile assumption. As shown in Figure 1, the pile vertical displacement vector can be decomposed into two directions, utilizing a coordinate system in which the y_0 axis represents the normal direction to the slope of the pile body. A dynamic Winkler model with four springs is then proposed, with both lateral and vertical springs, along with dashpots at the pile side and end. It is important to note that the pile is subdivided into frustum segments, with the number of segments n determined by the number of soil segments.

The tapered pile is generally made of concrete or steel material, which has a small damping coefficient relative to the soil, so the damping coefficient of the pile can be ignored. And assuming the pile segment i has a vertical displacement w_i, the vertical vibration differential equation of the pile can be derived from the force equilibrium analysis of the tapered pile unit, given by the following:

$$m_{pi}\frac{\partial^2 w_i(z,t)}{\partial t^2} - E_p A_{pi}\frac{\partial^2 w_i(z,t)}{\partial z^2} + p_{ni}\sin\theta + p_{si}\cos\theta = 0 \tag{1}$$

$$p_{si} = (k_{vi} + i\omega c_{vi})w_i(z,t)\cos\theta \tag{2}$$

$$p_{ni} = (k_{pi} + i\omega c_{pi})w_i(z,t)\sin\theta \tag{3}$$

where p_{si} is the shear force of the pile segment i, and p_{ni} is the normal force of the pile segment i. E_p, m_{pi}, and A_{pi} denote the pile elastic modulus, mass, and the cross-section area for segment i. To simplify, m_{pi} and A_{pi} are computed with the central cross-section of

the pile segment, as both the mass and cross-sectional area of the tapered pile vary with depth z.

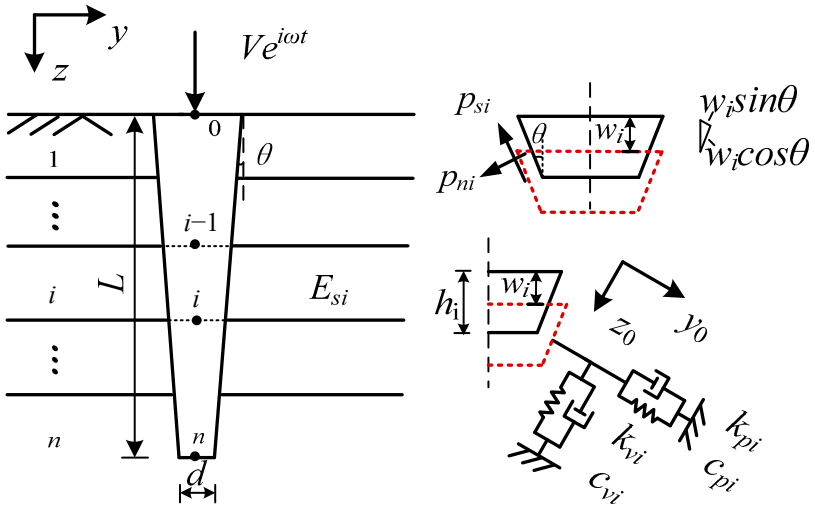

Figure 1. Analytical model for vertical vibration of a tapered pile.

The dynamic impedance of vertical and lateral springs considering pile–soil interaction, including stiffness and damping, can be determined by the formula below [19–21]

$$k_{vi} \approx 0.6E_{si}\left(1 + \frac{1}{2}\sqrt{a_{0i}}\right) \tag{4}$$

$$c_{vi} \approx 2\beta_{si}\frac{k_{vi}}{\omega} + \pi\rho_{si}V_{si}d_i a_{0i}^{-\frac{1}{4}} \tag{5}$$

$$k_{pi} \approx 1.2E_{si} \tag{6}$$

$$c_{pi} \approx 2\beta_{si}\frac{k_{pi}}{\omega} + 6\rho_{si}V_{si}d_i a_{0i}^{-\frac{1}{4}} \tag{7}$$

where the E_{si}, ρ_{si}, and β_{si} represent the soil elastic modulus, soil density, and soil damping at layer i, respectively. a_{0i} represents the dimensionless frequency, calculated by $\omega d_i/V_{si}$, where d_i, V_{si}, and ω are the diameter of the pile segment i, the shear wave velocity of soil at layer i, and the circular frequency of excitation force, respectively.

For steady vertical vibration, substituting $w_i(z,t) = w_i(z)e^{i\omega t}$ into Equation (1), the dynamic equilibrium equation for the ith pile unit can be calculated as follows:

$$\frac{d^2w_i(z)}{dz^2} + \left(\frac{\lambda_i}{h_i}\right)^2 w_i(z) = 0 \tag{8}$$

$$\lambda_i = h_i\left[\left(m_{pi}\omega^2 - \left[\left(k_{vi} + i\omega c_{vi}\right)\cos^2\theta + \left(k_{pi} + i\omega c_{pi}\right)\sin^2\theta\right)/E_pA_{pi}\right]^{1/2}\right. \tag{9}$$

For the ith pile segment, the displacement and axial force relationship between the endpoints of pile segment $i-1$ and i can be calculated from the unit force equilibrium, given as follows:

$$\begin{Bmatrix} w_i \\ N_i \end{Bmatrix} = [t^w]_i \begin{Bmatrix} w_{i-1} \\ N_{i-1} \end{Bmatrix} \tag{10}$$

$$[t^w]_i = \begin{bmatrix} \cos\lambda_i & \frac{h_i\sin\lambda_i}{E_pA_{pi}\lambda_i} \\ -\frac{E_pA_{pi}\lambda_i\sin\lambda_i}{h_i} & \cos\lambda_i \end{bmatrix} \tag{11}$$

where w_i and w_{i-1} are the vertical displacements of the base center and top center of pile segment i, respectively. N_i and N_{i-1} represent the axial force of the base center and top center of pile segment i, respectively.

Combined with Equation (11), the formula between the vertical displacement and the axial force at the node of pile head and pile end can be determined using the impedance function transfer matrix method, as follows:

$$\begin{Bmatrix} w_L \\ N_L \end{Bmatrix} = [T^w] \begin{Bmatrix} w_0 \\ N_0 \end{Bmatrix} \tag{12}$$

$$[T^w] = [t^w]_n [t^w]_{n-1} \cdots [t^w]_1 = \begin{bmatrix} T^w_{11} & T^w_{12} \\ T^w_{21} & T^w_{22} \end{bmatrix} \tag{13}$$

where w_L and w_0 are the vertical displacement at the base center and top center of the tapered pile, respectively. Similarly, N_L and N_0 are the axial force of the base center and top center of the tapered pile, respectively. T^w_{11}, T^w_{12}, T^w_{21}, and T^w_{22} are the four sub-matrices of the impedance function matrix $[T^w]$.

The vertical displacement w_L and axial force N_L can be determined through the solution of axisymmetric vertical vibration in a homogeneous, fully elastic half-space containing a rigid disk embedded at its surface [22].

$$N(L) = K_b w(L) = -\frac{d}{2} G_b (C_{w1} + iC_{w2}) w(L) \tag{14}$$

where K_b is the foundation stiffness, G_b is the shear modulus of soil at the pile end, C_{w1} and C_{w2} are the damping factors of the soil at the pile end. The values of C_{w1} and C_{w2} are related to the soil Poisson's ratio and can be found in Table 1 [23]. It can be calculated using the interpolation method when the soil's Poisson's ratio is not equal to 0, 0.25, or 0.5.

Table 1. The damping factors C_{w1} and C_{w2} for different soil Poisson's ratio.

ν	C_{w1} and C_{w2}
0	$C_{w1} = 4.0 - 0.0835a_0 + 0.6346a_0^2 - 2.6a_0^3 + 1.801a_0^4 - 0.3646a_0^5$
	$C_{w2} = 3.438a_0 + 0.5742a_0^2 - 1.154a_0^3 + 0.7433a_0^4$
0.25	$C_{w1} = 5.37 + 0.364a_0 - 1.41a_0^2$
	$C_{w2} = 5.06a_0$
0.5	$C_{w1} = 8.0 + 2.18a_0 - 12.63a_0^2 + 20.73a_0^3 - 16.47a_0^4 + 4.458a_0^5$
	$C_{w2} = 7.4148a_0 - 2.986a_0^2 + 4.34a_0^3 - 1.782a_0^4$

By substituting Equation (14) into Equation (12), the dynamic impedance of the tapered pile under vertical loading vibration can be derived as follows:

$$\Gamma_v = \frac{N(0)}{w(0)} = -\frac{T^w_{11} K_b + T^w_{21}}{T^w_{12} K_b + T^w_{22}} = K_v + iC_v \tag{15}$$

where Γ_v is the dynamic impedance of the pile at the pile head under vertical loading vibration, K_v is the vertical dynamic stiffness and C_v is the dynamic damping coefficient of the tapered pile, respectively.

3. Analyzing the Lateral Dynamic Characteristics of Tapered Piles in Layered Soils

Similarly, assuming the tapered pile is elastic, vertical, and fully bound to the soil. The pile length, pile diameter, and taper angle of the tapered pile are characterized by L d, and θ, respectively. The pile is assumed to be exposed to sinusoidal harmonic excitation

$He^{i\omega t}$ and $Me^{i\omega t}$. Considering the combined action of the shear and normal force due to the slope of the pile, the soil surrounding the pile shaft was considered to be continuous springs and dashpots and was decomposed into two directions. The dynamic Winkler four-spring model for lateral dynamic analysis presented in this paper is shown in Figure 2. It is important to note that the tapered pile is subdivided into frustum segments, with the number of segments n determined by the number of soil layers.

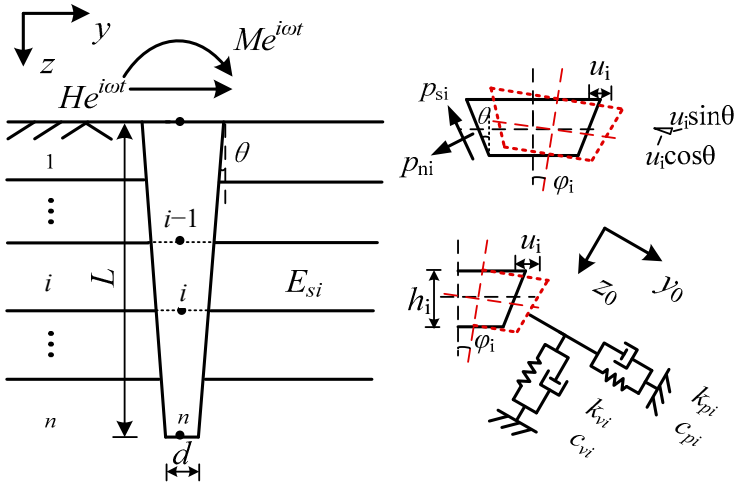

Figure 2. Analytical model for lateral vibration of a tapered pile.

Similarly to the tapered pile under vertical vibration, the damping of the pile is also neglected in the lateral vibration analysis. And assuming the pile segment i has a lateral displacement u_i, the tapered pile is divided into frustum segments, the differential equation of the tapered pile under lateral vibration can be derived from the force equilibrium analysis of the tapered pile unit, given as follows:

$$m_{pi}\frac{\partial^2 u_i(z,t)}{\partial t^2} + E_p I_{pi}\frac{\partial^4 u_i(z,t)}{\partial z^4} + p_{ni}\cos\theta + p_{si}\sin\theta = 0 \tag{16}$$

$$p_{si} = (k_{vi} + i\omega c_{vi})u_i(z,t)\sin\theta \tag{17}$$

$$p_{ni} = (k_{pi} + i\omega c_{pi})u_i(z,t)\cos\theta \tag{18}$$

where the p_{si}, p_{ni}, and I_{pi} are the shear force, normal force, the mass moment of inertia of the tapered pile segment i, respectively. E_p is the pile elastic modulus.

For lateral steady vibration, substituting $u_i(z,t) = u_i(z)e^{i\omega t}$ into Equation (18), the derivation procedures for dynamic equilibrium governing the i-th tapered pile segment can be established as follows:

$$\frac{\partial^2 u_i(z)}{\partial z^4} - \left(\frac{\lambda_i}{h_i}\right)^2 u_i(z) = 0 \tag{19}$$

$$\lambda_i = h_i[(m_{pi}\omega^2 - [(k_{vi} + i\omega c_{vi})\sin^2\theta + (k_{pi} + i\omega c_{pi})\cos^2\theta)/E_p I_{pi}]^{1/4} \tag{20}$$

For the ith pile segment, the displacement, rocking angle, lateral force, and bending moment relationship between the two endpoints of pile segment $i-1$ and i can be computed as follows:

$$\begin{Bmatrix} u_i & \varphi_i & H_i & M_i \end{Bmatrix}^{\mathrm{T}} = [t^u]_i \begin{Bmatrix} u_{i-1} & \varphi_{i-1} & H_{i-1} & M_{i-1} \end{Bmatrix}^{\mathrm{T}} \tag{21}$$

$$[t^u]_i = \frac{1}{2}\begin{bmatrix} ch\lambda_i + \cos\lambda_i & k_1(sh\lambda_i + \sin\lambda_i) & k_3(sh\lambda_i - \sin\lambda_i) & k_2(ch\lambda_i - \cos\lambda_i) \\ \frac{sh\lambda_i - \sin\lambda_i}{k_1} & ch\lambda_i + \cos\lambda_i & \frac{k_3(ch\lambda_i - \cos\lambda_i)}{k_1} & \frac{k_2(sh\lambda_i + \sin\lambda_i)}{k_1} \\ \frac{sh\lambda_i + \sin\lambda_i}{k_3} & \frac{k_1(ch\lambda_i - \cos\lambda_i)}{k_3} & ch\lambda_i + \cos\lambda_i & \frac{k_2(sh\lambda_i - \sin\lambda_i)}{k_3} \\ \frac{ch\lambda_i - \cos\lambda_i}{k_2} & \frac{k_1(sh\lambda_i - \sin\lambda_i)}{k_2} & \frac{k_3(sh\lambda_i + \sin\lambda_i)}{k_2} & ch\lambda_i + \cos\lambda_i \end{bmatrix} \quad (22)$$

where k_1, k_2, and k_3 are the normalized functions related to pile characteristics, and can be expressed as $k_1 = -h_i/\lambda_i$, $k_2 = {h_i}^2/(E_p I_{pi} {\lambda_i}^2)$ and $k_3 = {h_i}^3/(E_p I_{pi} {\lambda_i}^3)$, respectively.

By combining this with Equation (24), the formula between displacement, rocking angle, lateral force, and bending moment at the pile head and end can be derived using the transfer matrix method, as follows:

$$[T^u] = [t^u]_n [t^u]_{n-1} \cdots [t^u]_1 = \begin{bmatrix} T^u_{11} & T^u_{12} \\ T^u_{21} & T^u_{22} \end{bmatrix} \quad (23)$$

$$\begin{Bmatrix} u_L \\ \varphi_L \end{Bmatrix} = [T^u_{11}] \begin{Bmatrix} u_0 \\ \varphi_0 \end{Bmatrix} + [T^u_{12}] \begin{Bmatrix} H_0 \\ M_0 \end{Bmatrix} \quad (24)$$

$$\begin{Bmatrix} H_L \\ M_L \end{Bmatrix} = [T^u_{21}] \begin{Bmatrix} u_0 \\ \varphi_0 \end{Bmatrix} + [T^u_{22}] \begin{Bmatrix} H_0 \\ M_0 \end{Bmatrix} \quad (25)$$

where u_L, φ_L, H_L, and M_L are the lateral displacement, rocking angle, lateral loading, and bending moment of the bottom center of the pile, respectively. u_0, φ_0, H_0, and M_0 are the lateral displacement, rocking angle, lateral loading, and bending moment of the top center of the tapered pile, respectively. T^u_{11}, T^u_{12}, T^u_{21} and T^u_{22} are the four sub-matrices of the impedance function matrix $[T^u]$.

Hu et al. [24] pointed out that when the pile length L exceeds 10~15 times pile diameter d, The fixed boundary at the end of the pile or the free boundary at the end of the pile has little effect on the pile head impedance. In engineering practice, the pile length L typically exceeds 10~15 times pile diameter d. Therefore, assuming the pile end was fixed during the lateral excitation, then both u_L and φ_L are equal to 0. The dynamic impedance Γ_h under lateral loading vibration and the rocking dynamic impedance Γ_r under bending moment vibration of the tapered pile at the pile head can be derived as follows:

$$\Gamma_h = \frac{H_0}{u_0} = \frac{H_0}{f^s(1,1)H_0 + f^s(1,2)M_0} = K_h + iC_h \quad (26)$$

$$\Gamma_r = \frac{M_0}{\varphi_0} = \frac{M_0}{f^s(2,1)H_0 + f^s(2,2)M_0} = K_r + iC_r \quad (27)$$

where $[f^s]$ is the flexibility matrix at the pile head. K_h and K_r are the lateral and rocking dynamic stiffness, respectively. C_h and C_r are the lateral and rocking dynamic damping of the tapered pile, respectively.

4. Verification and Comparison

4.1. Comparison Against Equal Diameter Piles

Kaynia [25] calculated the dynamic stiffness and the dynamic damping of a vertically loaded cylindrical pile foundation in the elastic half-space using the boundary element method, and the research results were regarded as a rigorous solution. Figure 3 presents a comparison of the vertical dynamic stiffness and dynamic damping at the pile head between the results from Kaynia [25] and the simplified approach. Here, the taper angle of the pile is equal to 0°, length–diameter ratio L/d of the pile is equal to 15. The elastic

modulus ratio Ep/Es and density ratio ρ_s/ρ_p between the pile and soil are set as 1000 and 0.7, and the soil damping ratio β is assumed to be 5%. The vertical dynamic impedance function of the pile, Γ_v, is normalized by dividing the vertical static stiffness $k_{v,static}$ of the pile. The figure shows that the results from the simplified approach align with the rigorous results from Kaynia [25] across different frequency ranges.

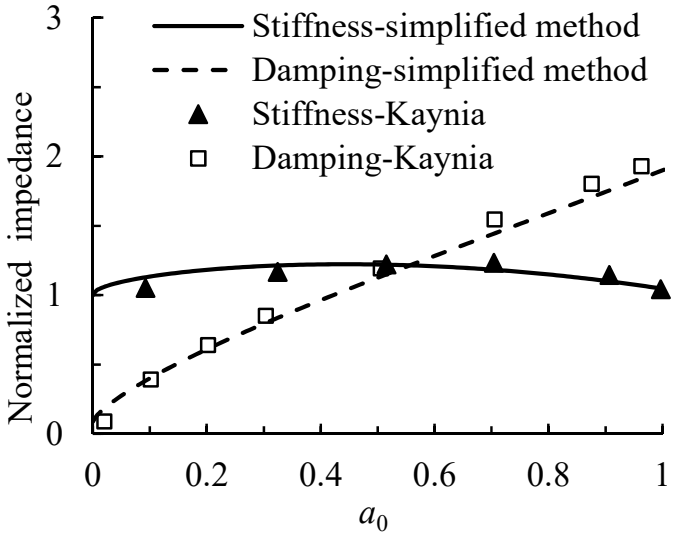

Figure 3. Normalized vertical dynamic impedances versus the dimensionless frequency of a single cylindrical pile.

Mylonakis and Gazetas [26] presented the results of the lateral dynamic impedance of a single cylindrical pile in a double-layer soil foundation, the pile length–pile diameter ratio and the soil depth of surface layer–pile diameter ratio are L/d = 20, h_1/d = 1.5, respectively. The elastic modulus and density ratios of the pile to soil are E_p/E_{s1} = 875, E_p/E_{s2} = 21, ρ_p/ρ_s = 1.5, and the soil damping ratio β = 5%. Similarly, the simplified method was applied to calculate the cylindrical pile in a double-layer soil foundation, and the lateral dynamic impedance Γ_h was normalized by dividing $E_{s1}d$, according to the results from Mylonakis and Gazetas [26] is satisfactory, as depicted in Figure 4.

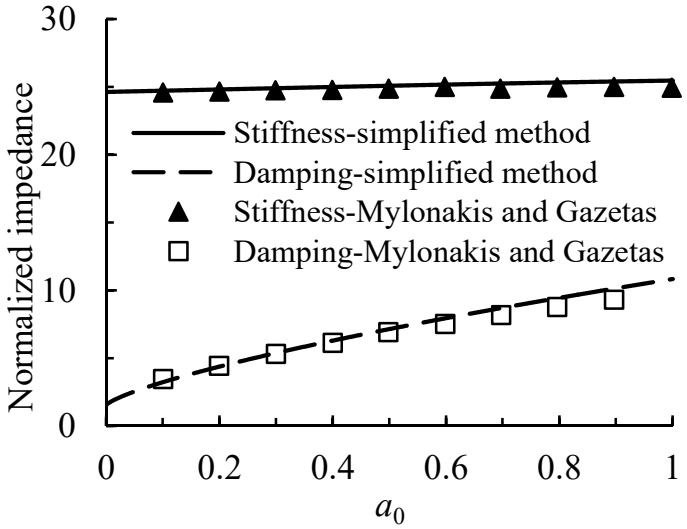

Figure 4. Normalized lateral dynamic impedances versus the dimensionless frequency of the cylindrical pile.

4.2. Comparison Against Tapered Piles

Ghazavi [27] performed a finite element model to analyze the dynamic axial loaded tapered pile, in which the pile parameters and soil parameters are shown in Table 2.

Table 2. Tapered pile and soil parameters.

Pile length	5 m
Equivalent Radius r_{eq}	0.1 m
Radius r_0 at pile head	0.16 m
Taper angle θ	1.5°
Elastic modulus of pile	20 GPa
The mass density of the pile	2400 kg/m^3
Elastic modulus of soil	30.6 MPa
Soil density	1800 kg/m^3
Soil Poisson's ratio	0.25

The equivalent radius of the tapered pile is given as follows:

$$r_{eq}^2 = \frac{1}{3}(r_0^2 + r_0 r_t + r_t^2) \tag{28}$$

where r_0 and r_t are the radius at the pile head and pile end, respectively.

The dimensionless amplitude A_w of the pile is defined as follows:

$$A_w = \frac{\omega^2}{\sqrt{\left(\frac{K_v}{M} - \omega^2\right)^2 + \left(\frac{C_v}{M}\right)^2}} \tag{29}$$

where ω is the circular frequency of vibration force and M is the additional mass at the pile head. K_v is the vertical dynamic stiffness of the pile and C_v is the vertical dynamic damping of the pile.

The normalized deformation amplitude at the top of the tapered pile for different loading excitation frequencies is given in Figure 5. Both end-bearing and friction piles were considered in this section, and the results of the simplified method were compared with those of the finite element model. Given that the reliability of the transfer matrix method depends on the way in which the pile section and the soil body are segmented, the effect of soil segments on the vertical dynamic response has been discussed. The results from the finite element method validate the overall predictions of the simplified method under a small number of soil segments, and the accuracy increases with increasing soil segments n. On the other hand, Figure 5 demonstrates that the results obtained using the proposed method align closely with those from the finite element method when the number of soil segments n equals 20. It should be noted that the computational efficiency is not significantly reduced when n = 20 relative to n = 5. In contrast to the idealization step structure ignoring the tapered angle effect [11], n needs to be close to 100, and the calculation accuracy will be satisfied. It is obvious that the calculation efficiency is significantly improved.

Few studies were conducted on the dynamic properties of the tapered piles under lateral vibration loading. Therefore, the proposed simplified method is validated through comparative analysis with the dynamic finite element model with a sponge boundary [28]. For a tapered pile (θ = 1.5°) subjected to lateral harmonic excitation, the mesh of the finite element model is illustrated in Figure 6. The wave reflection back into the region of the interesting part (white part) can be absorbed when the region of the sponge (gray part) has a high damping coefficient. The basic parameters of the sponge region are kept almost the same as those of the soil. The damping is simulated by Rayleigh damping and increases

gradually with distance to avoid any reflection caused by unexpected changes in the soil impedance. The pile and soil properties are given as: $L/r_0 = 20$, $E_p/E_s = 1000$, $\rho_p/\rho_s = 1.5$, $\beta = 5\%$, $E_p = 20$ GPa, and $r_0 = 0.5$ m.

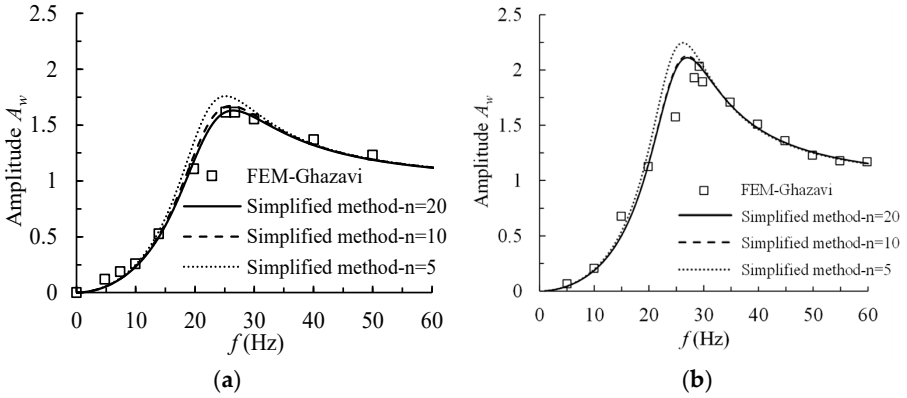

Figure 5. Dynamic vertical response of the tapered pile ($\theta = 1.5°$): (**a**) end-bearing pile; (**b**) friction pile.

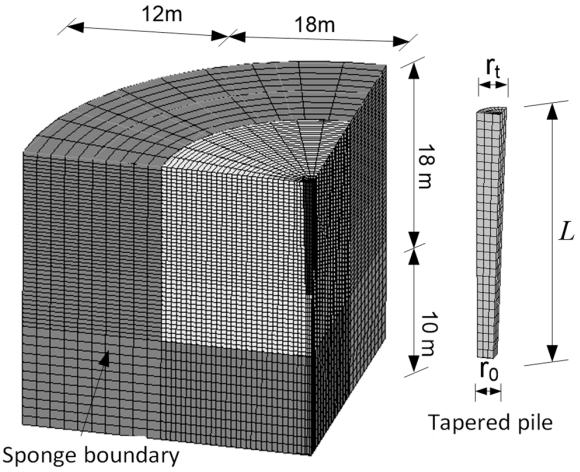

Figure 6. Finite element mesh of tapered pile ($\theta = 1.5°$).

The lateral dynamic impedance Γ_h was normalized by dividing by $2E_s r_{eq}$, and compared with those from the FEM as shown in Figure 7. The results show that satisfactory calculation accuracy is achieved when n is close to 20, verifying the efficiency and rationality of the proposed simplified approach. However, the results also show that increasing the number n to improve the accuracy of lateral dynamic impedance is not obvious.

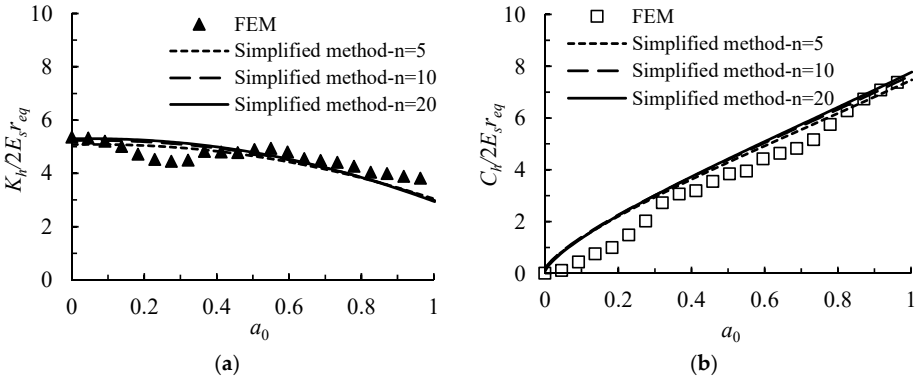

Figure 7. Lateral dynamic impedance of tapered pile ($\theta = 1.5°$): (**a**) dynamic stiffness; (**b**) damping.

5. Parametric Analysis

Unlike the cylindrical pile with a constant diameter, the geometric feature of the tapered pile is characterized by a progressive change in pile diameter from the head to the end of the pile, and the degree of change is controlled by the taper angle. Additionally, considering that soil is typically layered in engineering practice, two types of typical soil foundations (upper hard and lower weak, and upper weak and lower hard) are analyzed, and the dynamic properties of the tapered pile in these layered foundations are examined.

5.1. Effect of the Taper Angle on Dynamic Impedance

Soil properties and geometric parameters of tapered piles are as follows: elastic modulus ratio E_p/E_s = 1000, density ratio ρ_p/ρ_s = 1.5, length–diameter ratio L/r_{eq} = 30, pile elastic modulus E_p = 20 GPa, and pile length L = 15 m. In order to study the effect of taper angle on dynamic stiffness and dynamic damping, the dynamic characteristics of three kinds of tapered piles with taper angles θ equal to 0°, 1.5°, and 3° were first calculated and analyzed for comparison [7]. To ensure that the tapered piles have the same volume at different taper angles, the radius of the pile head and pile end were calculated using Equation (28).

The effect of the taper angle θ on the vertical dynamic impedance of the tapered pile is depicted in Figure 8. The number n of soil segments is equal to 20. The results show that the dynamic stiffness and dynamic damping decrease with decreasing taper angle. Nevertheless, the overall increase amplitude is relatively small. This indicates that with increasing taper angle θ leading to pile end diameter reduction, the magnitude of dynamic impedance increases along the pile shaft until it becomes comparable to the corresponding decrease at the pile end.

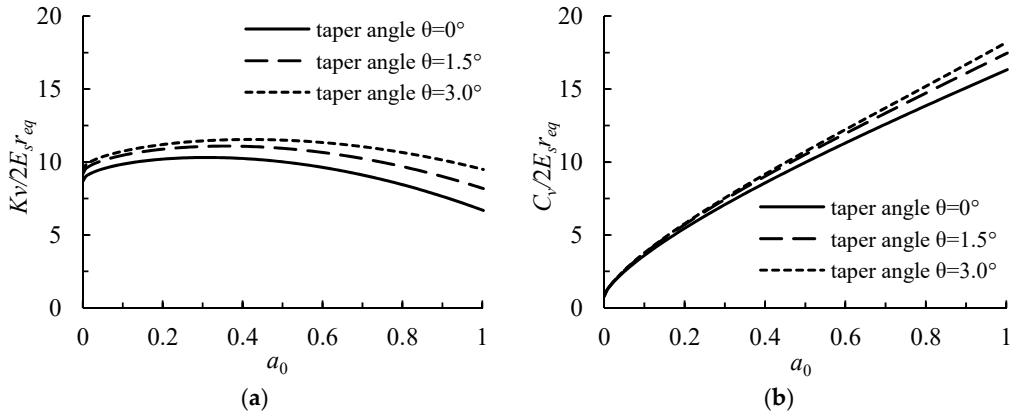

Figure 8. Effect of taper angle on the vertical dynamic properties: (**a**) dynamic stiffness; (**b**) damping.

Figures 9 and 10 show the effects of the taper angle θ on the lateral dynamic stiffness and damping of the tapered pile. The results demonstrate that the change in dynamic impedance pattern is in the same trend as that of Figure 8, where the lateral and rocking dynamic properties both increase with increasing taper angle, and the increase in lateral dynamic impedance is greater than that of vertical dynamic impedance, particularly for the rocking stiffness. The lateral stiffness of the lateral dynamic impedance increases by approximately 200~300% from taper angle θ = 0° to 3° when the a_0 is in the range of 0~0.2. However, the gap in dynamic stiffness decreases gradually at higher dimensionless frequencies. Meanwhile, the lateral stiffness decreases as the dimensionless frequency a_0 increases, while the rocking dynamic stiffness is slightly influenced by the a_0. The results also indicate that the lateral dynamic impedance of a tapered pile is greatly affected by the geometric feature of the pile. Specifically, a larger diameter near the pile head improves

the lateral dynamic impedance, assuming other conditions remain constant. This may be attributed to the fact that the dynamic impedance is closely related to the stiffness of the pile foundation. For vertically vibrating pile foundations, the dynamic impedance is affected by the axial stiffness $EA(z)$, but the dynamic impedance of laterally vibrating pile foundations relies on the moment of inertia of the pile section, $I(z)$, which is second to the fourth power of the depth, and a change in the taper angle apparently exacerbates the change in the bending stiffness $EI(z)$. In the meantime, vertical vibration propagation in the soil is dominated by compression wave (P-wave), and the wave velocity is determined by the elastic modulus of the pile body and the soil density, whereas horizontal vibrations manifest as shear wave (S-wave) whose propagation characteristics depends on $I(z)$ and soil shear modulus. This fundamental difference in wave mechanics also explains why taper angle exerts more pronounced influences on horizontal vibration behavior than vertical dynamics.

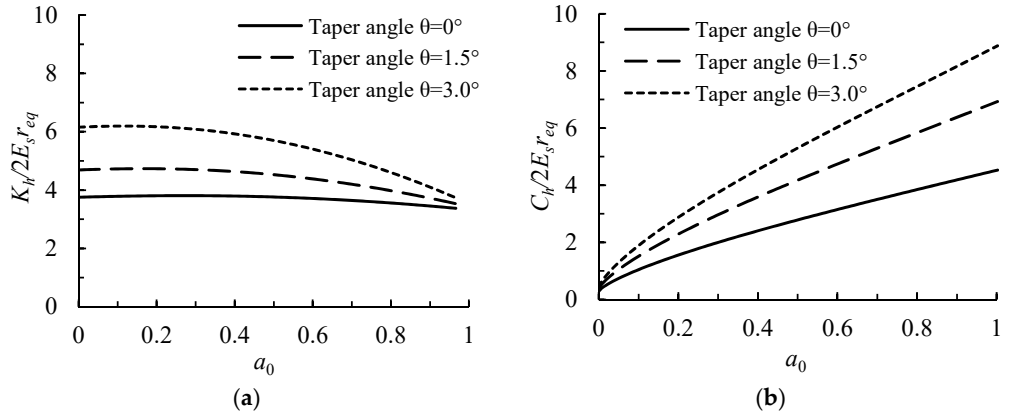

Figure 9. Effect of taper angle on lateral dynamic properties: (**a**) dynamic stiffness (**b**) damping.

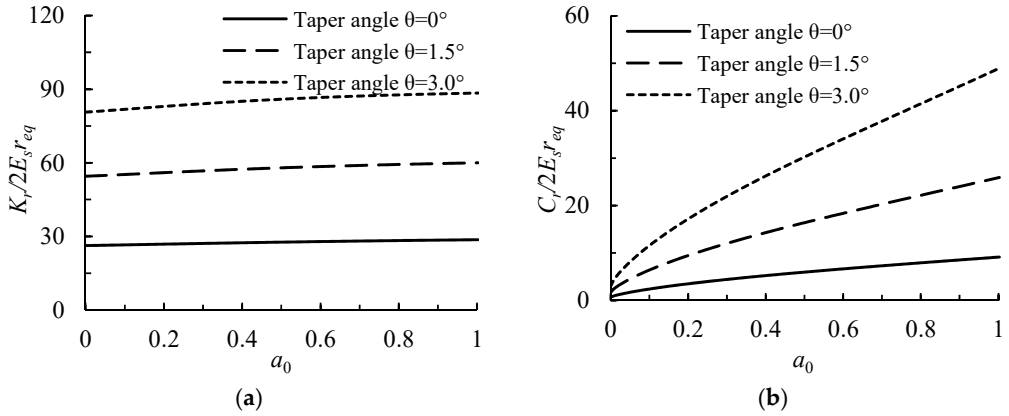

Figure 10. Effect of taper angle on rocking dynamic properties: (**a**) dynamic stiffness; (**b**) damping.

Therefore, the taper angle can be set to a relatively small value when the vertical dynamic characteristics of the pile foundation are mainly considered, while the taper angle can be set to a larger value for the pile foundation mainly subjected to lateral dynamic loading. It is also possible to set the tapered piles in a stepped shape by increasing the taper angle on the upper part of the pile in order to improve the lateral dynamic stiffness. However, it is important to note that the taper angle cannot be increased indefinitely, as increasing the taper angle accelerates the reduction in the pile end diameter, which also alters the vertical loading characteristics of the pile foundation.

5.2. Effect of Soil Layer Distribution on Dynamic Impedance

The effect of two typical double-layer soil foundations is discussed in this section, as demonstrated in Figure 11. The tapered pile (θ = 1.5°) was adopted to study the dynamic impedance. Other parameters of piles and soils are identical to those in Section 5.1.

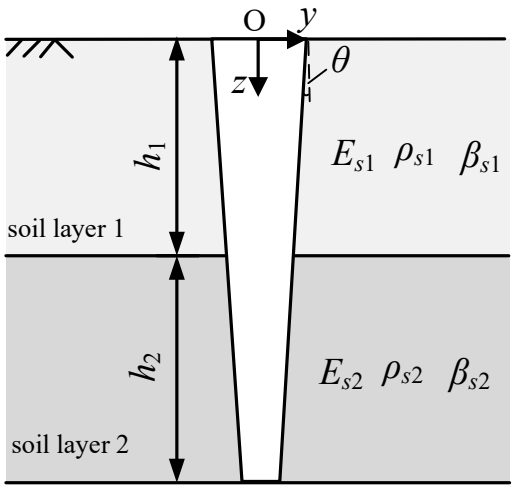

Figure 11. Illustration of double-layer soil foundations (case HW: upper hard and lower weak layered soil h_1/h_2 = 1.0, E_{s1}/E_{s2} = 4, E_p/E_{s2} = 1000; case WH: upper weak and lower hard layered soil h_1/h_2 = 1.0, E_{s1}/E_{s2} = 0.25, E_p/E_{s1} = 1000).

Figure 12 illustrates the correlation between soil properties and vibrational characteristics of vertically loaded tapered piles. The results show that increasing the soil elastic modulus around the pile side can significantly improve the vertical dynamic stiffness and dynamic damping of a single pile. Specifically, the vertical dynamic stiffness of the pile in double-layered soil is approximately twice that of homogeneous soil. The increase in vertical dynamic impedance due to the increasing elastic modulus of soil around the upper part of the pile is more pronounced than the increasing elastic modulus of soil around the lower part. It should be noted that the results are obtained based on the friction pile assumption. For end-bearing piles, the soil elastic modulus around the pile side is much smaller than the soil elastic modulus at the pile end, which may lead to different behaviors.

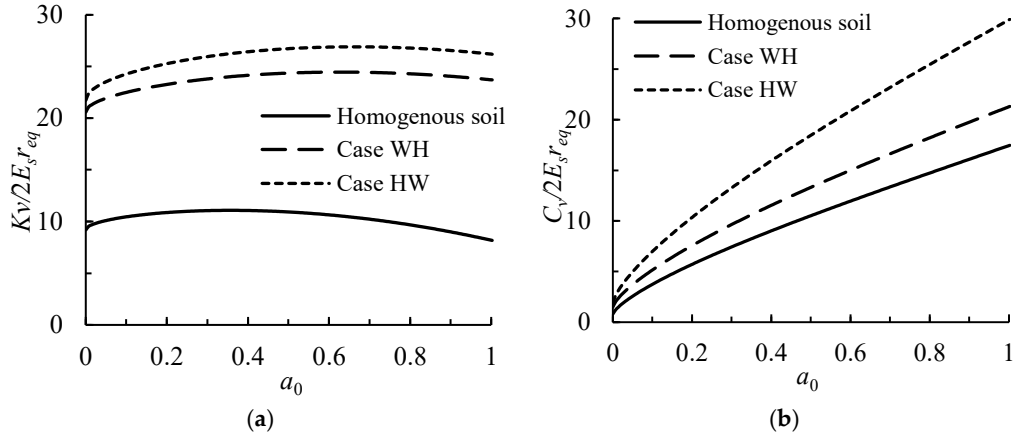

Figure 12. The vertical dynamic impedance of the tapered pile (θ = 1.5°): (**a**) dynamic stiffness; (**b**) damping.

Figures 13 and 14 demonstrate the effect of the soil properties on the dynamic impedance of the tapered pile under lateral vibration. The simulation results indicate that the lateral dynamic impedance characteristics of tapered pile foundations demonstrate

a proportional increase corresponding to the enhancement of elastic modulus in the surrounding soil medium. However, the increase in lateral dynamic stiffness is much greater in the upper hard and lower weak soil compared to the upper weak and lower hard soil. In particular, the lateral stiffness of lateral dynamic impedance in upper hard and lower weak soil increases by approximately 300% compared to that of homogenous soil. On the other hand, the rocking stiffness increases as the soil elastic modulus increases, while the rocking damping is less affected by the soil parameters. On the whole, parametric sensitivity analysis reveals that while the lateral dynamic impedance demonstrates marked susceptibility to soil parameter alterations, the rotational stiffness and damping components maintain relative insensitivity. Stratigraphic control mechanisms are principally governed by the upper soil stratum, accounting for a majority of the lateral and rocking dynamic impedance of the tapered pile.

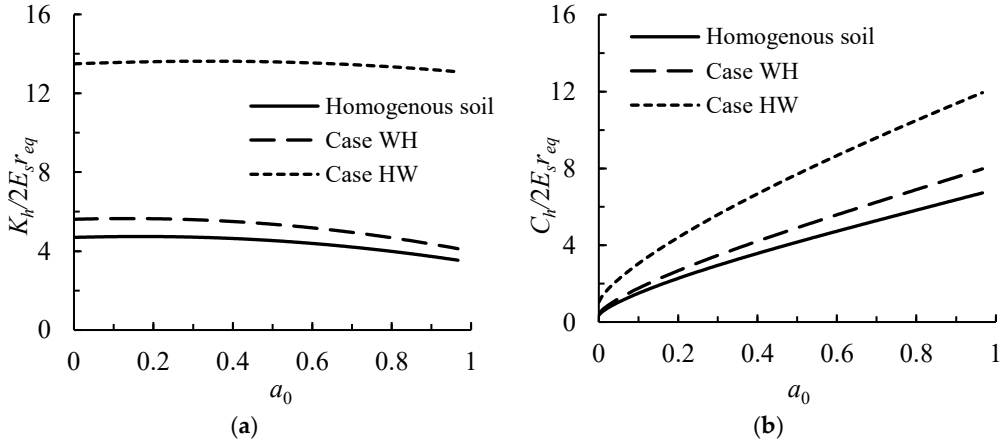

Figure 13. The lateral dynamic impedance of tapered pile in (θ = 1.5°): (**a**) dynamic stiffness; (**b**) damping.

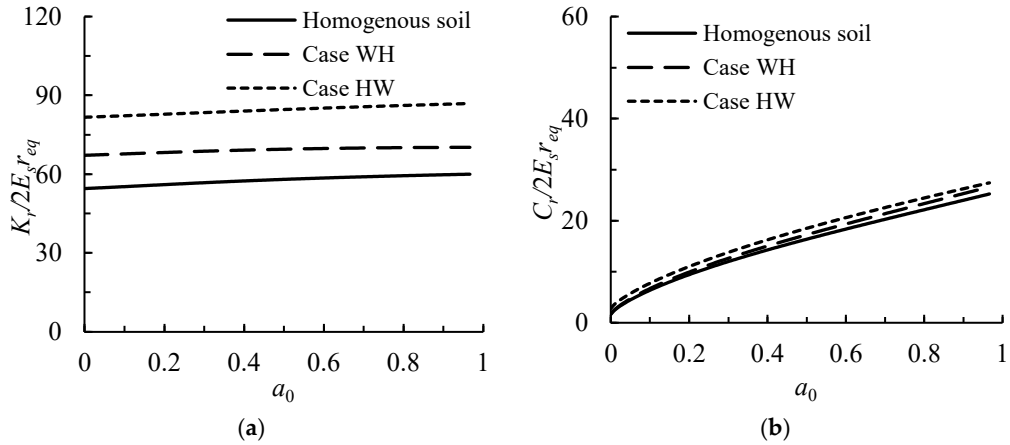

Figure 14. The rocking dynamic impedance of tapered pile (θ = 1.5°): (**a**) dynamic stiffness; (**b**) damping.

Therefore, strengthening the soil characteristics around the upper part of the pile helps to improve the vertical, lateral, and rocking impedance functions, especially for the vertical and lateral stiffness of the tapered pile, which can guide engineering practices. Regarding the engineering considerations of tapered pile configurations in civil engineering, the soil parameters surrounding the upper part of the tapered pile can be improved when the tapered pile is mainly subjected to vertical dynamic loading, and while the tapered pile foundation is mainly subjected to horizontal dynamic loading, the dynamic characteristics

can be improved from the taper angle and the soil properties surrounding the upper part of the pile.

6. Conclusions

This paper proposes a unified dynamic Winkler model for vertical and lateral dynamic analysis of tapered piles in layered soils using the impedance function transfer matrix method. The model can effectively account for the combined action of shear and normal force caused by the slope of the pile shaft which is different from the equal diameter pile assumption. Combined with the simplified method, the influences of dimensional parameters of the tapered pile and soil properties on the vertical, lateral, and rocking dynamic impedance of the tapered pile are discussed.

(1) The dynamic impedance of the tapered piles with equivalent volume under vertical vibration exhibits a positive correlation with taper angle enlargement, while both dynamic stiffness and damping of the tapered piles demonstrate a rate of increase that remains relatively modest.

(2) With an increase in the taper angle, the lateral and rocking dynamic impedance of the tapered pile with the same volume value increases more obviously than the vertical dynamic impedance. The lateral dynamic characteristics are more pronouncedly affected by the geometrical characteristics of the upper part of the pile. A larger diameter near the pile head results in better lateral dynamic impedance. It should be fully considered in subgrade treatment practice.

(3) The soil elastic modulus around the pile side can significantly improve the vertical dynamic impedance of the tapered pile. Specifically, the vertical dynamic stiffness of the tapered pile in double-layered soils is approximately twice that of homogeneous soil.

(4) Similarly, the lateral and rocking dynamic impedance of the tapered pile increases as the soil elastic modulus around the pile shaft increases. The increase in lateral dynamic stiffness is much larger in upper hard and lower weak soils than in upper weak and lower hard soils, while the rocking damping is less influenced by soil parameters.

(5) The soil parameters around the upper pile shaft are the primary factors affecting the vertical, lateral and rocking dynamic impedance of the tapered pile, which can guide engineering practice.

It should be declared that the frequency domain analysis method proposed in this study cannot effectively consider the nonlinear characteristics of foundations, including the cumulative strain effect of foundations under long-term cyclic loading [29,30]. For the case of large deformation, the equivalent nonlinear analysis theory based on the frequency domain method or the transient dynamic nonlinear analysis theory based on the time domain method can be further proposed to consider the nonlinear characteristics of the soil [31,32].

Author Contributions: Conceptualization, W.T.; software, Q.S. and H.X.; validation, H.X.; data curation, M.L. and N.S.; methodology, Q.S.; writing—original draft preparation, Q.S., H.X. and N.S.; writing—review and editing, W.T.; funding acquisition, and W.T. All authors have read and agreed to the published version of the manuscript.

Funding: This work was financially supported by the National Natural Science Foundation of China (Grant No. 52268069) and the Young Elite Scientists Sponsorship Program by CAST (Grant No. 2021QNRC001). These supports are gratefully acknowledged.

Data Availability Statement: Data are available upon reasonable request.

Conflicts of Interest: Author Mingkang Li was employed by the Xizang Boshi Engineering Design Co., Ltd. The remaining authors declare that the research was conducted in the absence of any commercial or financial relationships that could be construed as a potential conflict of interest.

References

1. Jiang, J.; Gao, G.; Gu, B. Comparison of belled pile, tapered pile and equal-diameter pile. *Chin. J. Geotech. Eng.* **2003**, *25*, 764–766.
2. Wei, J.; El Naggar, M.H. Experimental study of axial behavior of tapered piles. *Can. Geotech. J.* **1998**, *35*, 641–654. [CrossRef]
3. Hataf, N.; Shafaghat, A. Numerical comparison of bearing capacity of tapered pile groups using 3D FEM. *Geomech. Eng.* **2015**, *9*, 547–567. [CrossRef]
4. El Naggar, M.H.; Wei, J. Response of tapered piles subjected to lateral loading. *Can. Geotech. J.* **1999**, *36*, 52–71. [CrossRef]
5. Sakr, M.; El Naggar, M.H.; Nehdi, M. Lateral behaviour of composite tapered piles in dense sand. *Proc. Ins. Civ. Eng. Geotech. Eng.* **2005**, *158*, 145–157. [CrossRef]
6. Liu, J.; He, J.; Min, C. Study of the rational wedge angle in a composite foundation with rammed soilcement tapered piles. *Chin. Civ. Eng. J.* **2010**, *43*, 122–127. (In Chinese)
7. Shafaghat, A.; Khabbaz, H. Recent advances and past discoveries on tapered pile foundations: A review. *Geomech. Geoengin.* **2022**, *17*, 455–484. [CrossRef]
8. Saha, S.; Ghosh, D.P. Vertical vibration of tapered piles. *J. Geotech. Eng.* **1986**, *112*, 290–302. [CrossRef]
9. Wu, W.; Wang, K.; Dou, B. Vertical dynamic response of a viscoelastic tapered pile embedded in layered foundation. *J. Vib. Shock.* **2013**, *32*, 120–127. (In Chinese)
10. Wang, K.; Tong, W.; Xiao, C.; Wu, B. Study on dynamic response of tapered pile and model test. *J. Hunan Univ. (Nat. Sci.)* **2019**, *46*, 94–102. (In Chinese)
11. Cai, Y.; Yu, J.; Zheng, C.; Qi, Z.; Song, B. Analytical solution for longitudinal dynamic complex impedance of tapered pile. *Chin. J. Geotech. Eng.* **2011**, *33*, 392–398. (In Chinese)
12. Hu, J.; Tu, W.; Gu, X. A simple approach for the dynamic analysis of a circular tapered pile under axial harmonic vibration. *Buildings* **2023**, *13*, 999. [CrossRef]
13. Shua, Q.; Liu, K.; Li, J.; Tu, W. Time domain nonlinear dynamic analysis of vertically loaded tapered pile in layered soils. *Buildings* **2024**, *14*, 445. [CrossRef]
14. Ghazavi, M. Analysis of kinematic seismic response of tapered piles. *Geotech. Geol. Eng.* **2007**, *25*, 37–44. [CrossRef]
15. Dehghanpoor, A.; Ghazavi, M. Response of tapered piles under lateral harmonic vibrations. *Int. J. Geomate* **2012**, *2*, 261–265. [CrossRef]
16. Yang, Z.; Wu, W.; Lu, H.; Liu, H.; Zhang, Y. Horizontal vibration characteristics of tapered pile embedded in viscoelastic foundation. *J. Harbin Inst. Technol.* **2021**, *53*, 74–83. (In Chinese)
17. Zhou, H.; Kong, G.; Cao, Z. Theoretical analysis on pile-soil interaction of tapered pile under lateral load. *J. Cent. South Univ. (Sic. Technol.)* **2016**, *47*, 897–904. (In Chinese)
18. Huang, M.; Tu, W.; Gu, X. Time domain nonlinear lateral response of dynamically loaded composite caisson-piles foundations in layered cohesive soils. *Soil Dyn. Earthq. Eng.* **2018**, *106*, 113–130. [CrossRef]
19. Gazetas, G.; Makris, N. Dynamic pile-soil-pile interaction. Part I: Analysis of axial vibration. *Earthq. Eng. Struct. Div.* **1991**, *20*, 115–132. [CrossRef]
20. Makris, N.; Gazetas, G. Dynamic pile-soil-pile interaction. Part II: Lateral and seismic response. *Earthq. Eng. Struct. Div.* **1992**, *21*, 145–162. [CrossRef]
21. Deng, Q.; Tu, W.; Liu, L.; Zhang, P.; Liu, K. Horizontal nonlinear vibration response analysis of tapered pile in layered foundation. *J. Vib. Shock.* **2024**, *43*, 126–133. (In Chinese)
22. Novak, M.; Aboul-ella, F.; Nogami, T. Dynamic soil reactions for plane strain case. *J. Eng. Mech. Div.* **1978**, *104*, 953–959. [CrossRef]
23. Novak, M.; Beredugo, Y.O. Vertical vibration of embedded footings. *J. Soil. Mech. Found. Div.* **1972**, *98*, 1291–1310. [CrossRef]
24. Hu, F.; Xie, K.; Xiao, Z. Dynamic response analysis for a single pile subjected to lateral loading. *J. Zhejiang Univ.* **2003**, *37*, 420–425. (In Chinese)
25. Kaynia, A.M. Dynamic Stiffness and Seismic Response of Pile Groups. Ph.D. Thesis, Massachusetts Institute of Technology, Cambridge, MA, USA, 1982.
26. Mylonakis, G.; Gazetas, G. Lateral vibration and internal forces of grouped piles in layered soil. *J. Geotech. Geoenviron.* **1999**, *125*, 16–25. [CrossRef]
27. Ghazavi, M. Response of tapered piles to axial harmonic loading. *Can. Geotech. J.* **2008**, *45*, 1622–1628. [CrossRef]
28. Varun, D.; Assimaki, D.; Gazetas, G. A simplified model for lateral response of large diameter caisson foundations-Linear elastic formulation. *Soil Dyn. Earthq. Eng.* **2009**, *29*, 268–291. [CrossRef]
29. Zhang, Z.; Gao, W. Effect of different test methods on the disintegration behaviour of soft rock and the evolution model of disintegration breakage under cyclic wetting and drying. *Eng. Geol.* **2020**, *279*, 105888. [CrossRef]
30. Zhang, Z.; Gao, W.; Wang, X.; Zhang, J.; Tang, X. Degradation-induced evolution of particle roundness and its effect on the shear behaviour of railway ballast. *Transp. Geotech.* **2020**, *24*, 100388. [CrossRef]

31. Tu, W.; Gu, X.; Chen, H.; Fang, T.; Geng, D. Time domain nonlinear kinematic seismic response of composite caisson-piles foundation for bridge in deep water. *Ocean. Eng.* **2021**, *235*, 109398. [CrossRef]
32. Tu, W.; Huang, M.; Gu, X.; Chen, H. Nonlinear dynamic behavior of laterally loaded composite caisson-piles foundation under scour conditions. *Mar. Georesour. Geotec.* **2020**, *38*, 1265–1280. [CrossRef]